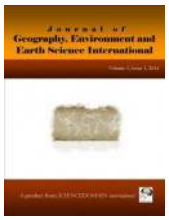

Journal of Geography, Environment and Earth Science International
6(4): 1-18, 2016; Article no.JGEESI.26110
ISSN: 2454-7352

SCIENCEDOMAIN *international*
www.sciencedomain.org

Examination of Land Surface Deformation in the Eastern Tennessee Seismic Zone (ETSZ) Using Persistent Scatterers Interferometric Synthetic Aperture Radar (PSInSAR)

Zhiming Yang[1*] and Abdella Salem[1]

[1]North Carolina Central University, Durham, NC 27707, USA.

Authors' contributions

This work was carried out in collaboration between both authors. Author ZY designed the study and wrote the first draft of the manuscript. Author AS managed the literature review and conducted data processing and analyses. Author ZY also supervised data processing and analysis and performed spatial analysis. Both authors read and approved the final manuscript.

Article Information

DOI: 10.9734/JGEESI/2016/26110
Editor(s):
(1) Iovine Giulio, CNR-IRPI (National Research Council-Institute of Research for the Geo-hydrologic Protection) of Cosenza, Italy.
(2) Tim G. Frazier, Department of Geography, Director - Hazards and Climate Impacts Research Center (HazCIRC), The State University of New York, Binghamton, USA.
(3) Ioannis K. Oikonomopoulos, Core Laboratories LP., Petroleum Services Division, Houston Texas, USA.
Reviewers:
(1) Ahmet Sayar, Kocaeli University, Turkey.
(2) Hongli Wang, National Center for Atmospheric Research, Boulder, CO, USA.
(3) Marcos Eduardo Hartwig, 725, Vila Clementino, 04027-000 Sao Paulo, SP, Brazil.
Complete Peer review History: http://sciencedomain.org/review-history/15267

Original Research Article

Received 1st April 2016
Accepted 25th June 2016
Published 2nd July 2016

ABSTRACT

Aims: The purpose of this study is to detect land surface deformation in the Eastern Tennessee Seismic Zone using persistent scatterers interferometric synthetic aperture radar technique.
Study Design: This study employed persistent scatterers interferometric synthetic aperture radar technique to analyze a series of ESA SAR images and derive surface deformation velocity along the slant range direction in Eastern Tennessee Seismic Zone which is the second most active seismic zone in the eastern United States.
Place and Duration of Study: Department of Environmental, Earth and Geospatial Sciences, North Carolina Central University, Services between June 2012 and July 2014.

**Corresponding author: E-mail: zyang@nccu.edu;*

Methodology: In this study, forty six ESR ½ SAR (SLC format) images covering two study areas with different seismic activity were inputted to ENVI/SARscape/Persistent Scatterers Stacking Interferometry Module with DEM (10-meter resolution) acquired from USGS. These SAR images cover a part of the ETSZ, with spatial extent between 35.118 and 36.824 degrees north in latitude, and between 83.707 and 84.871 degrees west in longitude and were acquired between 1992 and 1999. After interferometric SAR analysis, ArcGIS 10.2 software was used to conduct spatial statistics of surface deformation velocity along line of sight in both study areas and to examine the land surface deformation in cities located in the west and east of the New York-Alabama lineament.
Results: It was found that average uplift/subsidence velocity was higher in the study area which was more seismically active. Results also show that there was no significant difference in average uplift, subsidence and overall velocity between two sides of New York-Alabama lineament in ETSZ.
Conclusion: Our findings indicate that there is no direct association between the land surface deformation and the position relative to the NY-AL lineament in the study areas. However, interpretation of results from this study needs to be cautious since there are many factors, in addition to seismotectonic processes, that contribute to land surface deformation. Geodetic measurements such as ground leveling measurements are highly suggested in the ETSZ to verify finding from this study and to identify the deformation sources.

Keywords: PSInSAR; tectonic activity; uplift; subsidence; deformation.

1. INTRODUCTION

The Eastern Tennessee Seismic Zone (ETSZ), located west of the Blue Ridge Mountains and stretching from northern Alabama to southern West Virginia, is the second most active seismic zone in the eastern United States. Small earthquakes are felt in this region on average once a year and hundreds of earthquakes that cannot be felt have been recorded by seismic networks [1]. The largest historic earthquakes (magnitude 4.6) occurred in 1973 near Knoxville, Tennessee and on April 29, 2003 near Fort Payne, Alabama. The most recent earthquake of magnitude > 4 occurred on November 10, 2012 near Whitesburg, Kentucky. Studies of instrumental seismicity showed that New York-Alabama magnetic lineament is aligned with the modern seismicity of the ETSZ [2-4].

Spirit leveling, GPS, and extensometer measurements are widely used traditional methods for monitoring land surface changes. Only few land surface deformation studies have been completed in the central and eastern United States using these techniques. [5] employed leveling data to analyze relative rates of vertical crustal movement in the eastern United States and found that the Appalachian Highlands experienced uplift relative to the Atlantic Coast at a rate of up to 6 mm/year. [6] utilized leveling technique to detect surface deformation in the Blue Ridge and Piedmont provinces of North Carolina and Georgia along two leveling profiles. They reported that there was an increase in the uplift rate along the profile extending from Morristown, Tennessee, via Asheville, North Carolina, to Newton, North Carolina with the highest uplift rate of about 4.0±0.9 mm/year near Ashville NC, with respect to benchmarks near Morristown or Newton. Based on continuous GPS data [7] observed a vertical subsidence rate of up to 1.4 mm/year in the fore bulge with a maxima located about 2000 km from the glacial isostatic adjustment (GIA) center. They also concluded that no significant motion was detected in the New Madrid seismic zone (NMSZ) at a 95% confidence level. However, significant horizontal motions at rate 0.37±0.07 mm/year were discovered between two continuous GPS sites in NMSZ using leveling measurements; these motions might indicate a potential for M 7 earthquake on the shallow portion of the Reelfoot fault with recurrence times of about 500 years [8].

Synthetic Aperture Radar (SAR) is an active remote sensing technique in which SAR sensor transmits microwave signals whose wavelengths range from 1 mm to 1 m then records backscattered energy from targets at the ground surface and provides terrain structural information [9]. One of space-borne radar systems is the European Satellite Agency (ESA) ERS-2 satellite and it collects images with a 100 km wide swath at a constant off-nadir angle of around 21° (at mid-range). SAR systems record both amplitude and phase values, which depend both on the local reflectivity and on the sensor-target distance [10].

Interferometric Synthetic aperture Radar (InSAR) is a technique that employs phase information in

a pair of high resolution SAR images to provide elevation data [11]. The basic principle of InSAR is that sensor-target distance is measured by phase difference relative to two SAR images. In InSAR, "Each SAR image pixel represents the coherent sum of all scattering elements within a resolution cell and each element contributes both with its own complex reflectivity (amplitude and phase) and with its individual distance from the sensor" [10]. The phase of SAR images is affected by many factors including satellite orbit, topography and atmosphere. Once their contributions are removed, InSAR can be used measure surface deformation accurately.

Persistent Scatterers Interferometric Synthetic Aperture Radar (PSInSAR) is the most advanced SAR technique that performs surface deformation measurements on Persistent Scatterers (PS) using time-series SAR data while overcoming de-correlation effects. It allows monitoring ground deformation with a higher spatial resolution than current GPS or leveling techniques and has a potential to detect land displacement at a millimeter scale [12]. A PS point represents an object whose reflectivity does not vary with time and is much higher than any other surrounding objects within the same pixel [13]. PS points correspond to man-made structures such as buildings and roads, or solid natural surfaces such as exposed rocks and soil.

PSInSAR technique has been widely used in various earthquake-related studies. [14] employed PSInSAR to 30 ERS images covering the northern San Francisco Bay area and deformation (creep) rate was discovered of up to 6 mm/year. [15] reported a differential uplift of 1.4–1.7 mm/year across the Giudicarie belt in Italy after analyzing 80 ERS1 and ERS2 images covering the time period between 1992 and 1996. The displacement rate was estimated as 5.4 and 6 mm/year for Granada basin, Spain, using DePSI and StaMPS software package and 29 ERS-1/2 and 22 ENVISAT ASAR images [16]. [17] processed 21 ENVISAT images acquired for the period from June 2003 to November 2008 covering the islands of Cephalonia and Ithaca, Greece, and concluded that the uplift rate was 2–4 mm/year mainly along the southern and southeastern parts of the islands while larger velocities (>4 mm/yr) occurred at the western parts of islands. [18] stated that highest positive velocity value of 1.07±0.31 mm/year was found along the Cottian Alps/Po Plain boundary, Italy, after running PSINSAR on 163 ERS-1 and ERS-2 SAR images from May 1992 to January 2001. [19] analyzed postseismic deformation for the 1989 Mw 6.9 Loma Prieta earthquake using PSINSAR and obtained up to 2 mm/yr surface subsidence in the northern Santa Cruz Mountains between 1992 and 2002. These examples provide evidences that the PSInSAR technique can be successfully used to detect ground deformation associated with tectonic activity.

The purpose of this study was to detect land surface deformation in selected regions of ETSZ with different levels of seismic activity and explore the relationship between surface deformation and the NY-AL lineament using PSInSAR technique. The detection of land surface deformation in the ETSZ could improve our understanding of the intraplate seismicity and earthquake related hazards.

2. MATERIALS AND METHODS

2.1 Study Areas

The two study areas are shown on Fig. 1. There is a noticeable difference in the seismic activity between the two regions, region one being less seismically active due to its location on the periphery of the ETSZ. The selection was driven by the availability of the satellite images and the idea to examine the relationship between land surface deformation and levels of seismic activity.

2.2 Geological Setting and Soils

The ETSZ is an intraplate earthquake zone and there are no known active faults that reach the surface. Thus seismicity in this zone may not be related to the surface geology and the earthquakes originate below the Paleozoic formations [20]. The geological information about the study areas is displayed in Figs. 2.1 and 2.2. In the first study area, dominant rock types are Atokan and Morrowan Series, Cambrian and Ordovioian rocks. In the second study area, dominant rock types are Ordovioian, Cambrian and Z-sedentary rocks. The surface geologic formations in this area are characterized as Paleozoic sedimentary rocks [21], which are composed of sandstone, carbonate, and shale. The first study area is located within provinces of Appalachian Plateaus and Valley and Ridge while most of second study area is contained within the provinces of Valley and Ridge and Blue Ridge.

About 250 to 300 million years ago, North America and South America continents collided to create an supercontinent Pangea [22,23]. The formation of Pangea was accompanied by a major deformation event known as the Alleghanian Orogeny in the southern Appalachian region [24]. By the Late Triassic period the supercontinent Pangea started to break apart [23]. The recent stress field in east North America was caused by continental resistance to plate motion along the east coast of North America and it has been in place since the Cretaceous [25]. Seismicity in the ETSZ occurred within Precambrian basement rocks that were covered by younger Paleozoic sheets [3]. The recent seismicity indicates that the basement faults are being reactivated by modern stress field [22].

The Appalachians' ancient faults were developed during the formation of the Appalachian Mountains over several hundred million years [1]. Active faults in the Appalachian region are known to be developed beneath land surface. Magnetic measurements in the ETSZ have recognized a major potential field anomaly known as the New York-Alabama lineament, which is characterized by a high gradient from central Alabama through eastern Tennessee to New York. This lineament represents a major strike- slip fault in the basement roc k [25]. It extended for more than 1600 kilometers and may be associated with variations in structural or minerals composition of basement rocks [2].

In Eastern Tennessee, soils were developed mainly from sandstone and shale and there were also shallow and rocky soils [26]. Soils in the Great Valley were formed in residuum from limestone, sandstone, and shale. In some areas, there were mixtures of Reddish-Brown Lateritics and more prevalent Red-Yellow-Podzolic soils. Soils in Sequatchie Valley were mainly developed from old alluvium [26]. The rocks underneath soils include dolomite, shale, sandstone, and limestone bedrock, of Cambrian or lower Ordovician age [27].

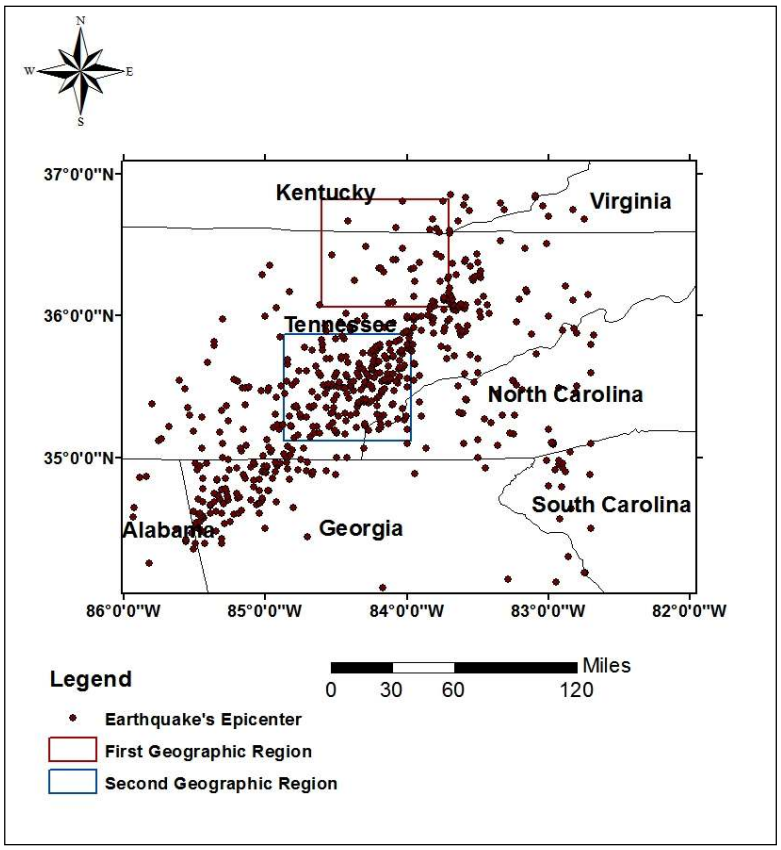

Fig. 1. Map of the study areas and earthquake epicenters between 1976 and 2008 in the ETSZ
[Data sources USGS and CEUS-SSC]

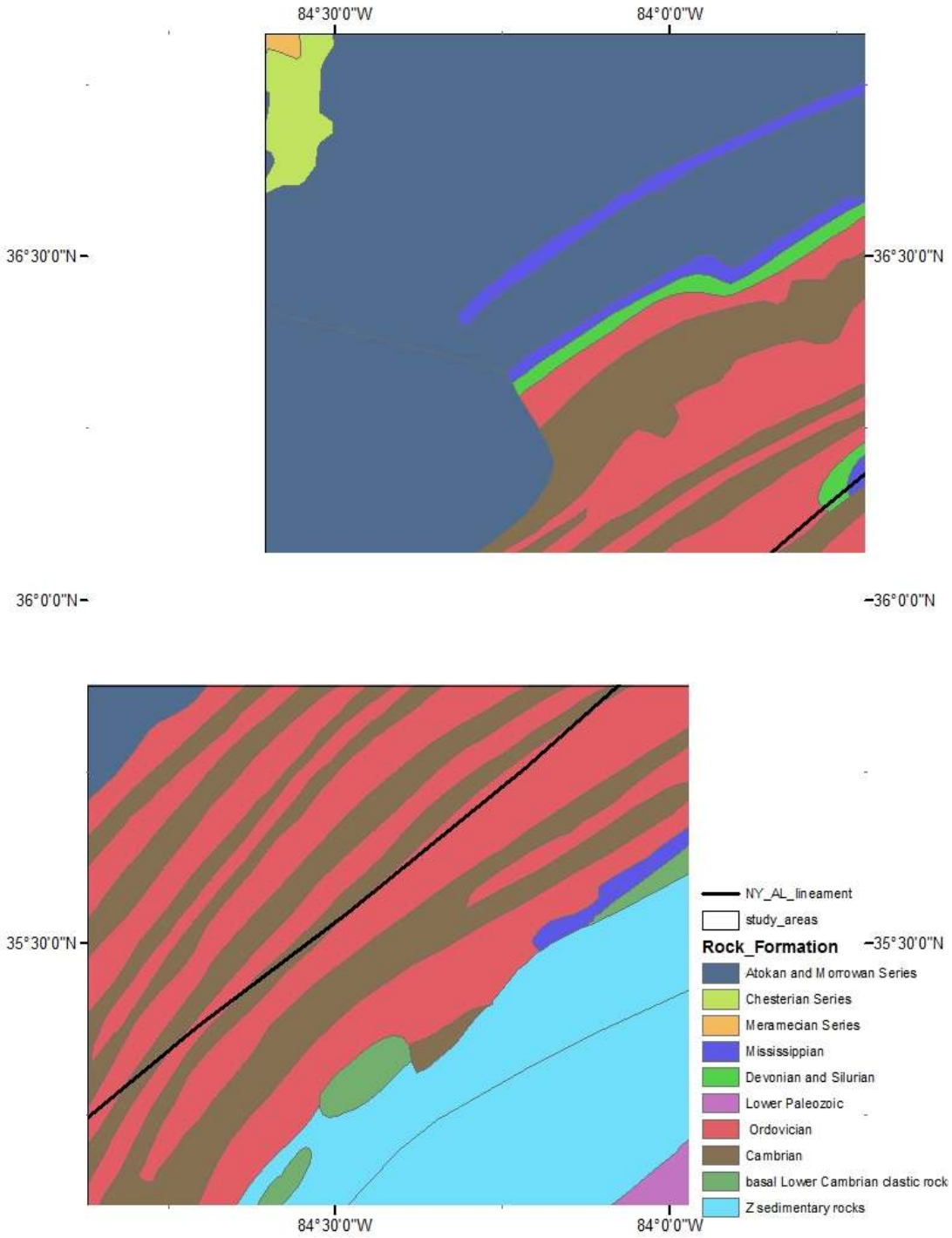

Fig. 2.1. Rock map of the study areas. Derived from a digital geologic map of the US states (USGS). Thick black line denotes NY-AL lineament southern segment after [4]

2.3 Data Acquisition

ERS-1 and -2 satellites were launched in 1991 and 1995 respectively by European Satellite Agency (ESA) to provide environmental monitoring in the microwave spectrum. They rotate around the Earth at about 800 km and were equipped two specialized radars (SAR) and

an infrared imaging sensor. The resolution of ERS imagery is about 5 m in azimuth direction and 9.5 m in slant range and 25 m in ground range [10].

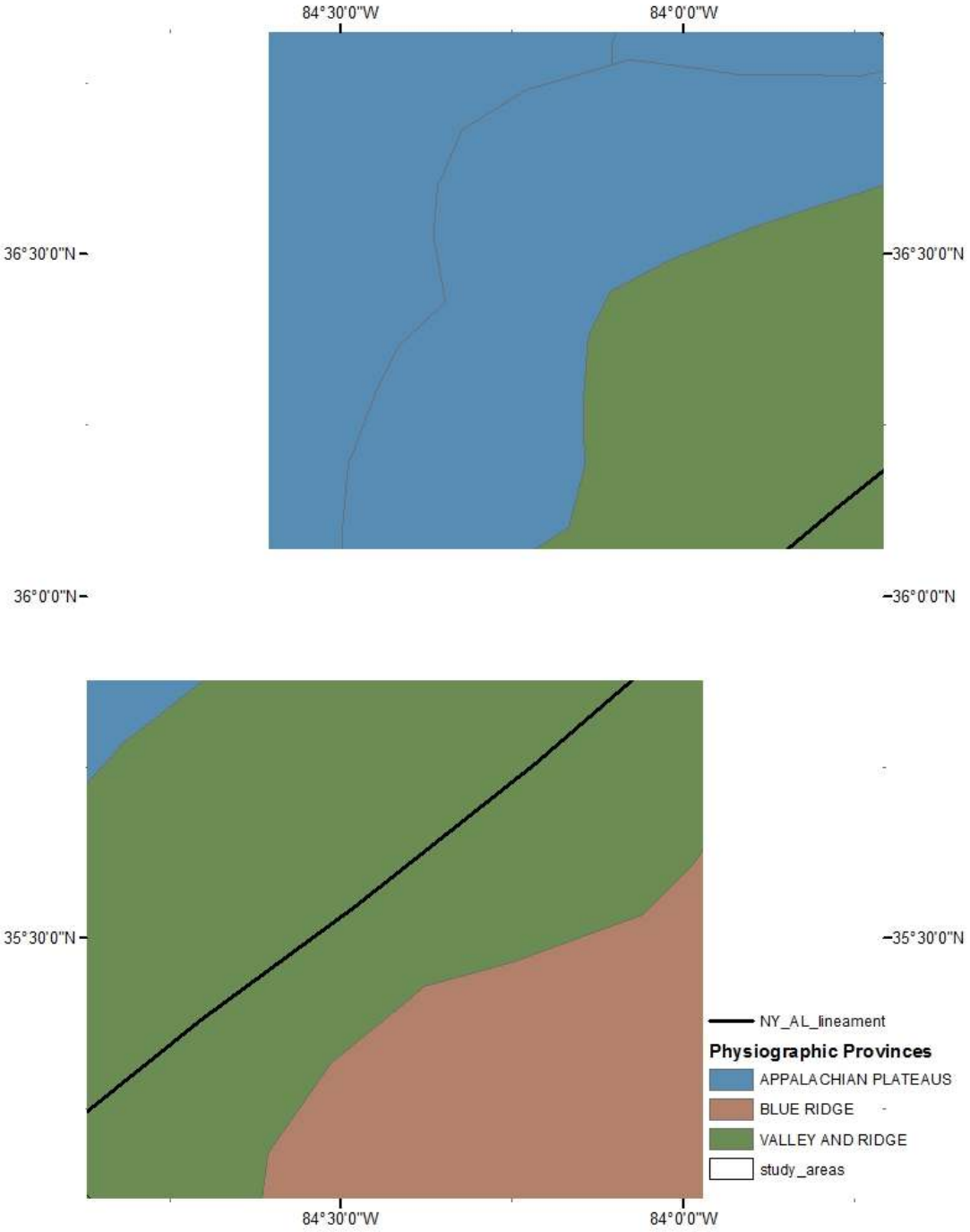

Fig. 2.2. Physiographic province map of the study areas. Derived from a digital physiographic province map of the US states (USGS). Thick black line denotes NY-AL lineament southern segment after [4]

Two sets of SAR imagery (ERS-1 and ERS-2, C band) were acquired from European Satellite Agency (ESA) and cover the time period between 1992 and 1999. First data set covers the first study area between 36.067 and 36.824 degrees north in latitude, and between 83.707 and 84.606 degrees west in longitude. The second data set covers the second study area located between 35.118 and 35.875 degrees north in latitude, and between 83.971and 84.871 degrees west in longitude. Orbital data for both satellites was also acquired from the ESA. The DEM data was downloaded from the USGS website and spatial resolution is 1/3 arc per second (approximately 10 meters).

2.4 Data Preprocessing

The interferometric baseline is defined as "the separation between two SAR antennas that receive echoes of the same ground area" [28]. It is composed of temporal baseline (day difference between consecutive images) and spatial baseline (difference between the positions of SAR antenna phase centers of satellite 1 and satellite 2) [29]. Critical baseline is maximum allowable baseline beyond which interferogram is completely decorrelated [30]. The critical baseline of the ERS SAR images is 1050 m.

Each raw ERS-1 or ERS-2 SAR image was imported to ENVI/SARscape [31] with correspondent orbit file and then converted to a SAR image in single looking complex (SLC) format. Spatial baseline was checked for each SAR image and images with a spatial baseline larger than five times that of a critical baseline were removed from each dataset based on ENVI help menu.

2.5 Data Processing

All selected SAR images in SLC format were uploaded as input to Interferometry Stacking (Persistent Scatterers) Module in ENVI 4.8/SARscape software. In total, 23 SAR images were used for the first study area and 22 SAR images were used for the second study area. First, the best combinations of master and slave images were identified by selecting automatic reference option for each SAR dataset. The image that has small spatial and temporal baseline with respect to the other images was selected as the master image and rest of the images were chosen as slave images. Each study area was further divided into two equal-sized sub-areas for each data set considering the processing limit of software. Region of interest was defined by uploading the vector file for each sub study area. The DEM of the region was uploaded as input to the Interferometry Stacking Module in order to remove the topographic phase contribution. After that, each stack of imagery was processed to calculate deformation velocity and total displacement using following steps:

(a) Images cutting and co-registration: pixels in the master image were aligned with corresponding pixels in the slaves' images.
(b) Flattened Interferogram generation: phase variation due slant range displacement was subtracted and removing topographic phase contribution was removed to generate flattened interferograms.
(c) Adaptive filter and coherent generation: phase noise was reduced in the flattened interferogram using an adaptive filter and the interferometric coherence was generated.
(d) Phase unwrapping: an integer multiple of 2π was subtracted or added to interferometric fringes to solve phase discontinuity and generate an elevation map.
(e) PS candidates' selection: the errors caused by orbital factors, topography and atmosphere were estimated and removed. Pixels with higher coherence than the amplitude average/standard deviation ratio (default 0.75) were selected as PS candidates.
(f) Phase to displacement: displacement along the slant range direction was computed.
(g) PS geocoding: three dimensional maps of an object's coordinates were changed to two dimensional maps. Both geocoded raster and vector files with parameters including mean velocity, displacement time series, and total displacement were generated. Mean intensity images and KML files were projected onto the cartographic system of the uploaded DEM. The precision of mean velocity is ±0.35 mm/year.
(h) For each study area two velocity shape files for each sub-area were merged into one shape file using ArcGIS 10.2 software.

2.6 Data Analysis

The data analysis for this study was mainly conducted for cities in two study areas since the PSInSAR technique provides highly reliable

results in non-vegetated areas (urban areas). The following data analyses were completed using ArcGIS 10.2 software [32]. 1) Spatial statistics was conducted to examine differences in average uplift, subsidence and overall velocity between the two study areas and a two-sample T-test was used to test significances of differences. In this T-test means of two normally distributed populations and t-statistics were calculated using designated formula; If the calculated t-statistic is greater than the critical t-value, the means of the two populations are considered as different statistically with certain confidence level [33]. T-test has been used in analysis of deformation data derived from InSAR to compare difference in surface deformation rate between two location/areas or time periods [34,35]. 2) PS shape files were intersected with a shape file of cities within two study areas and then a zonal statistics on velocity was done for each city/town in each study area. The average uplift, subsidence and overall velocity of all cities/towns in each study area was summarized and compared. A T-test was used to test significances of differences between two study areas and among cities. 3) Cities in each study area were divided into two sub-areas based on their location relative to the NY-Alabama lineament. For a city/town that is bisected by the NY-Alabama lineament such as Knoxville and Athens TN, PS points were separated into the western and eastern side based on their location. The average of uplift, subsidence and overall velocity in the western and eastern sides of NY-Alabama lineament were calculated for each side of area and compared. In addition, the spatial correlation between the distance of city center to the NY-Alabama lineament and their average velocity was examined to further explore the impact of the lineament on the land surface deformation. The main purpose of these analyses was to examine the spatial difference in deformation velocity along line of sight (LOS) between the two sides of NY-Alabama lineament in order to help understand the relationship between land surface deformation and the position relative to the NY-AL lineament in the study areas.

3. RESULTS AND DISCUSSION

3.1 Regional Land Surface Deformation

Spatial-statistics of velocity (LOS) for each study area was conducted and results were summarized in Table 1. The T-test was conducted to examine differences in mean uplift and subsidence between the two study areas.

Table 1 shows that more PS points were detected in the second study area than in the first study area. This is because there are larger urban areas in the second study area than in the first study area and more scatterer points were detected. As mentioned before, PS points correspond to man-made structure such as buildings and roads which are mainly located in urban areas.

T-test indicated that there was a significant difference in uplift and subsidence rate between the two study areas at 95% confidence level. It can be seen that the average uplift and subsidence rates were lower in the first study area than in the second study area. This may be related to the difference in seismic characteristics of each study area as the second area has higher rate of seismic activity than the first study area.

In both study areas, there were more PS points experiencing uplift than subsidence. Thus regionally both study areas experienced uplift for the time period between 1992 and 1999. This result is similar to findings from [5,6] but opposite to the finding from [7]. The later could be due to

Table 1. Spatial statistics of land deformation for two study areas

	First study area	Second study area
Total number of images co-registered to the master image	23	21
Total number of detected PS points	10137	60628
Total PS points experiencing uplift	5141	30656
Average uplift rate (mm/year)	3.55 mm/year	4.18 mm/year
Uplift standard deviation	2.05	2.44
Total PS points experiencing subsidence	4996	29972
Average subsidence rate (mm/year)	-3.41 mm/year	-4.13 mm/year
Subsidence standard deviation	2.03	2.41

the difference in the extent of the study area and the method used; their study area covered the U.S continent and the subsidence rate at 1.4 mm/year was an interpolated value from many GPS sites.

In addition, a significant variation in surface deformation rate including outliers (higher or lower values) was found in both study areas. This might be due to the fact that many factors can contribute to land surface deformation in those areas. For land subsidence, it might be related to many geological events such as groundwater withdrawal, erosion, karst subsidence and landslide. Karst landscape is very common in many parts of the eastern Tennessee [36]. In eastern Tennessee, it was estimated that there were 300 subsidence events at more than 200 sites between 1982 to 1986 [37]. Also, surface erosion might be an important contributing factor. Tennessee ranks the first in erosion rate of cultivated cropland among the 50 states [38]. Thus no clearly defend spatial pattern was observed in the two study areas.

3.2 The Land Surface Deformation for Cities in Two Study Areas

The spatial statistics of land surface deformation for cities in the study areas is summarized in Table 2, and showed in Figs. 4 and 5 below. In the first study area, except in Norris, TN, there were more PS points experiencing uplift than subsidence and the similar uplift rate was also observed ranging from 3.51 to 3.91 mm/year. Large differences in subsidence rates were found among cities in the first study area and they ranged from -2.67 mm/year in Middlesborough and Williamsburg, KY, to -3.79 mm/year in La Follette, TN. In the second study area, except in Madisonville, and Sweetwater, TN, there were more PS points experiencing uplift than subsidence. The close uplift rate was also observed ranging from 3.69 to 4.05 mm/year. Slightly larger differences in subsidence rate were found among cities in the second study area and they ranged from -3.89 mm/year in Cleveland, TN, to -4.50 mm/year in Etowah, TN. No consistent spatial pattern in uplift or subsidence rate was found in each study area among cities or within each city. Instead, a similar variation in uplift and subsidence as those of the study area level was also found at a city level which can both be explained by many factors contributing to land surface deformation in those cities in eastern Tennessee.

Table 2 shows that much more PS points were detected for cities in the second study area than in the first study area. This is because there are larger cities in the second study area than in the first study area and thus more scatterer points were detected. It can also be seen that more PS points experienced uplift than subsidence in both study areas suggesting that both study areas experienced uplift regionally for the time period between 1992 and 1999. This result is again consistent to the findings by [5,6].

The T-test shows that both average uplift and subsidence velocities were lower for cities in the first study area than for those in the second study area at 95% confidence level. This is the same result as the comparison at the study area level mentioned in the last section suggesting that more seismically active region (second study area) experienced more deformation including land uplift or subsidence.

Additionally, it was noticed that average uplift velocity in the two study areas was 3.52 and 4.06 mm/year, respectively, while their average subsidence velocity was 3.47 and 4.11 mm/year, respectively. These values are very similar to the values at a study area level: average uplift velocity was 3.55 and 4.18 mm/year, respectively, while average subsidence velocity was 3.41 and 4.13 mm/year, respectively, in the first and second study area. This indicate land uplift/subsidence rates in cities in each study area are sufficient to represent land uplift/subsidence rates in their study area although PS points in those cities account for a smaller portion of all PS points in their correspondent study area. Thus, it is practical and valid to use land uplift/subsidence information in cities in each study area to represent land uplift/subsidence information in the whole study area in later analysis.

To understand the impact of rock type on land surface deformation, PS points were superimposed on the geological map of the study areas (Fig. 6). In the first study area, most PS points are over Ordovioian rock (Table 3). There were few PS points over Atokan and Morrowan Series, Cambrian and Devonian and Silurian and Ordovioian rocks. Mean uplift and subsidence rate was 3.62 and 2.82 mm/year over Atokan and Morrowan Series and 3.76 and 3.75 mm/year over Cambrian rock respectively. Mean uplift and subsidence rate was 3.94 and 3.89 mm/year over Devonian and Silurian rock and

3.63 and 3.53 mm/year over Ordovioian rock respectively. No significant difference in deformation rate was found among different rock types.

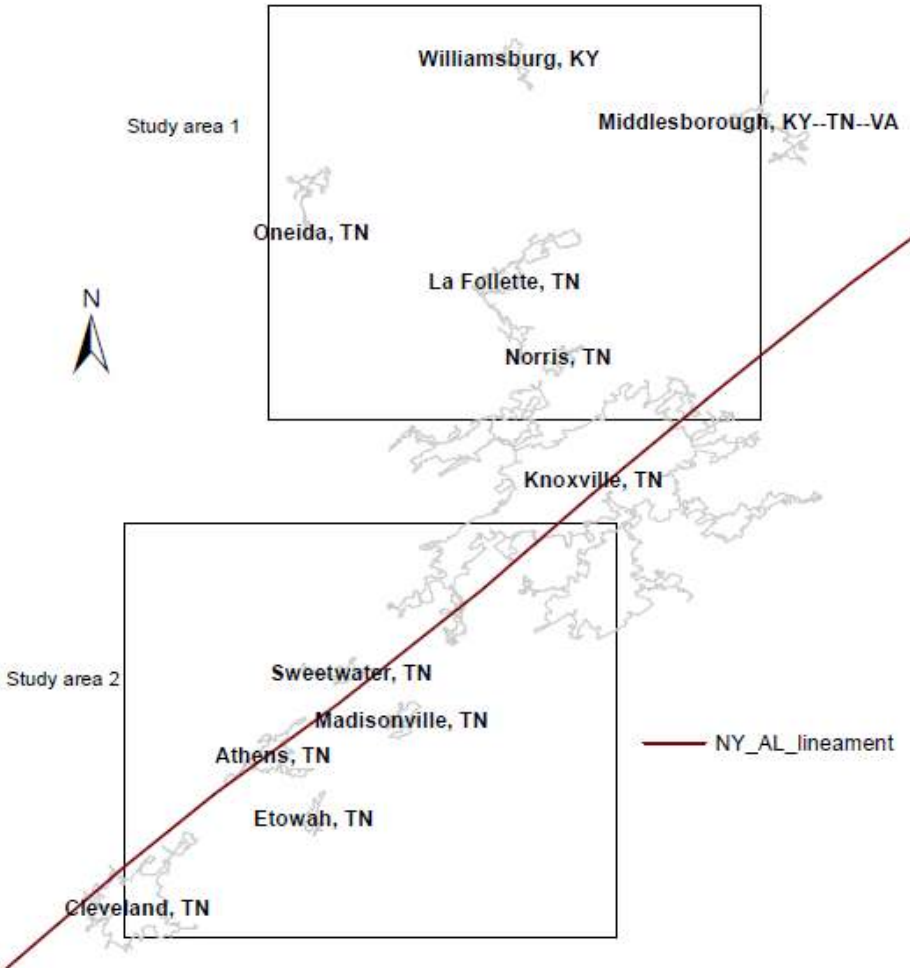

Fig. 3. Map of cities in the study areas

Table 2. Land surface deformation velocity (mm/year) in cities in two study areas

Name	Uplift			Subsidence			Overall		Study area
	#PS	M_V	Std.	#PS	M_V	Std.	M_V	Std.	
Knoxville, TN(north)	103	3.64	2.07	85	-3.50	2.08	0.41	4.12	First
Middlesborough, KY-TN-VA'	25	3.51	2.26	12	-2.67	1.84	1.51	3.59	First
La Follette, TN	79	3.81	2.12	71	-3.79	2.10	0.21	4.34	First
Norris, TN	4	0.96	0.81	11	-3.33	1.74	-2.18	2.45	First
Oneida, TN	23	3.91	1.96	9	-2.84	1.75	2.01	3.58	First
Williamsburg, KY	18	3.52	1.70	10	-2.67	1.73	1.31	3.42	First
First study area	253	3.64	2.09	198	-3.47	2.05	0.52	4.10	
Knoxville, TN(south)	453	4.05	2.50	442	-4.26	2.49	-0.05	4.84	Second
Athens, TN	208	4.40	2.41	189	-4.26	2.49	0.28	4.97	Second
Cleveland, TN	634	4.00	2.42	575	-3.89	2.38	0.25	4.61	Second
Madisonville, TN	78	3.96	2.45	83	-4.18	2.53	-0.24	4.77	Second
Sweetwater, TN	75	4.16	2.42	78	-4.24	2.23	-0.13	4.80	Second
Etowah, TN	64	3.69	2.46	57	-4.50	2.24	-0.17	4.71	Second
Second study area	1512	4.06	2.45	1424	-4.11	2.43	0.10	4.76	

#PS: Number of PS points; M_V: Average velocity; Std: Standard deviation

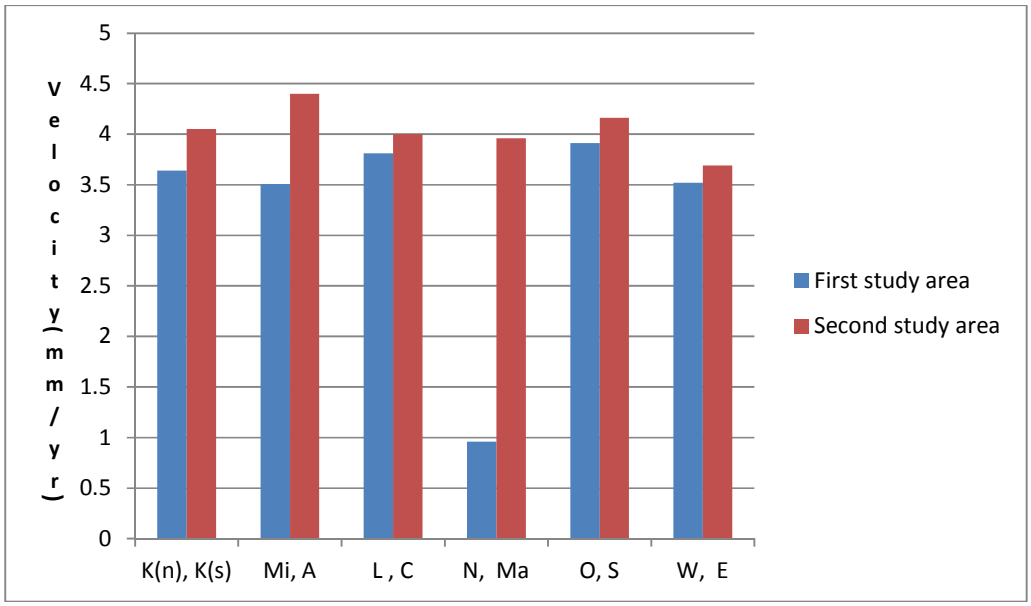

Fig. 4. Mean uplift velocity in the two study areas (K(n): Knoxville (north); K(s): Knoxville (south); Mi: Middlesborough; A; Athens; L: La Follette; C: Cleveland; N: Norris; Ma: Madisonville; O: Oneida; S: Sweetwater; W: Williamsburg; E: Etowah)

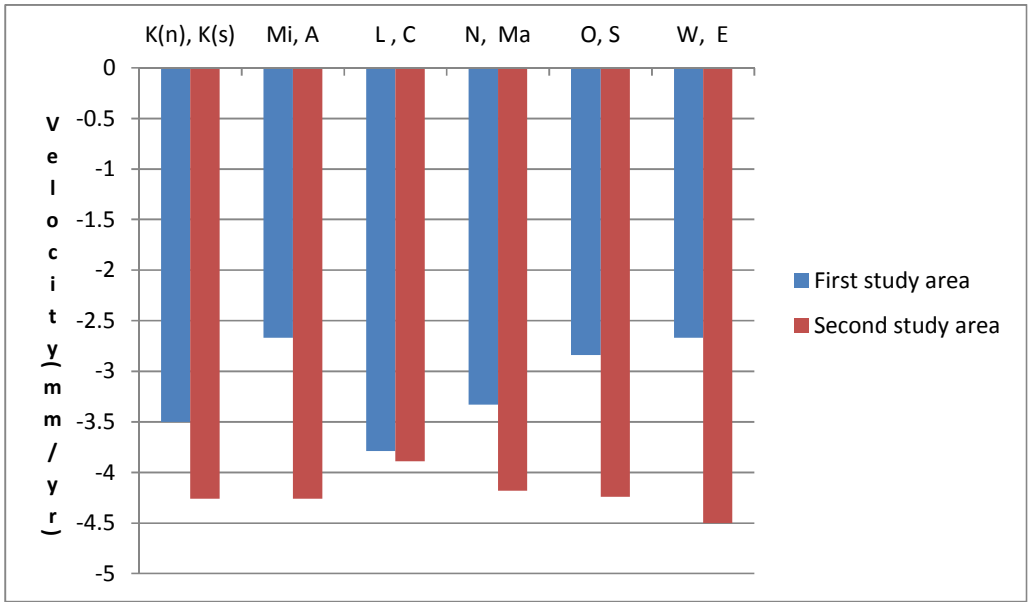

Fig. 5. Mean subsidence velocity in the two study areas (K(n): Knoxville(north); K(s): Knoxville(south); Mi: Middlesborough; A; Athens; L: La Follette; C: Cleveland; N: Norris; Ma: Madisonville; O: Oneida; S: Sweetwater; W: Williamsburg; E: Etowah)

In the second study area, PS points were over Ordovioian rocks and Cambrian rocks (Table 3). There were little more PS points over Ordovioian rocks than Cambrian rocks. Mean uplift and subsidence rate was 3.93 and 4.16 mm/year over Ordovioian rock respectively. Mean uplift and subsidence rate was 4.21 and 4.11 mm/year over Cambrian rock respectively. No significant difference in deformation rate was discovered between two different rock types.

Compared to the first study area, surface deformation rate was higher in the second area regardless of rock types. This supports the conclusion that surface deformation is associated with levels of seismicity in study areas since there was high level of seismicity in the second study area than in the first study area.

3.3 Spatial Pattern of Land Surface Deformation in Two Sides of NY-Alabama Lineament

The surface deformation velocities for cities were summarized for western urban area and eastern urban area separately (Table 4). Mean uplift and subsidence velocity for cities at each side of NY-Alabama lineament is shown in Figs. 7 and 8. In the area west of NY-AL lineament, except in Norris, TN, the uplift rate ranged from 3.51 to 4.54 mm/year among cities. Large differences in subsidence rate were found among cities and they ranged from -2.67 mm/year in Middlesborough and Williamsburg, KY to -4.24 mm/year in Sweetwater, TN. In the area east of NY-AL lineament the close uplift rate was also observed ranging from 3.69 to 4.27 mm/year. Slightly larger differences in subsidence rate were found among cities and they ranged from -3.89 mm/year in Cleveland, TN, to -4.66 mm/year in Knoxville (NE), TN. Again, no consistent spatial pattern in uplift or subsidence rate was found on either side of NY-Alabama lineament among cities. Instead, there were significant variation in uplift and subsidence among cities in each side of the NY-AL Lineament.

The T-test shows that there were no significant differences in uplift, subsidence and overall velocity between urban areas west and east of NY-AL lineament at 95% confidence level. The T-test also shows that there were no significant differences in uplift, subsidence and overall velocity between western and eastern Knoxville and Athens, TN, at 95% confidence level. Thus it is clear that there is no direct association between the position relative to the NY-AL lineament and the land surface deformation in the study areas.

Distances of city's geographic center to the NY-AL magnetic lineament were shown in Table 2. The spatial correlation test shows that there was no significant correlation between the distance of city center to the NY-Alabama lineament and the average uplift, subsidence and overall rate at 95% confidence level. This indicates that the surface deformation of cities in study areas was not spatially related to the NY-Alabama lineament.

The average surface deformation velocity values from this study were comparable to results from previous studies. This indicates PSInSAR technique is applicable to study of land surface deformation in ETSZ. The findings from this study could help understand the overall surface deformation in the region. However, no clear spatial patterns in uplift and subsidence velocity in the two study areas were detected. Higher velocity values in some locations might be due to the fact that those locations are mostly vegetated and the atmospheric contribution to the interferometric phase may not have been estimated accurately and removed completely. This is because atmospheric contribution is very hard to evaluate accurately in the areas where the density of strong scatterers is very low [12].

Many types of erosion such as rill erosion, gully erosion and splash erosion [39,40] move soil and weathered rock from one place to other locations and cause subsidence or uplift in land surface. The erosion can also have impact on the state of gravitational stresses in one area, leading to tectonic activity [41]. Many studies observed a relationship between water level decline and the rate of subsidence in various places due to substantial groundwater extraction for agricultural and municipal/industrial use [42,43]. In eastern Tennessee, Karst landscape is prone to create sinkholes where limestone, carbonate rock and salt beds below land are dissolved by acidic groundwater and cause dramatic land surface

Table 3. Land surface deformation velocity (mm/year) in cities over different rocks

Rock type	Uplift			Subsidence			Overall		Study
	#PS	M_V	Std.	#PS	M_V	Std.	M_V	Std.	area
Atokan and Morrowan Series	52	3.62	2.02	26	-2.81	1.80	1.47	3.61	First
Cambrian	48	3.76	2.14	38	-3.76	1.97	0.44	4.27	First
Devonian and Silurian	23	3.94	1.78	28	-3.90	2.31	-0.37	4.42	First
Ordovician	125	3.63	2.13	111	-3.53	2.09	0.27	4.15	First
Cambrian	667	4.22	2.43	612	-4.11	2.09	0.27	5.15	Second
Ordovician	748	3.93	2.47	735	-4.16	2.46	-0.08	4.74	Second

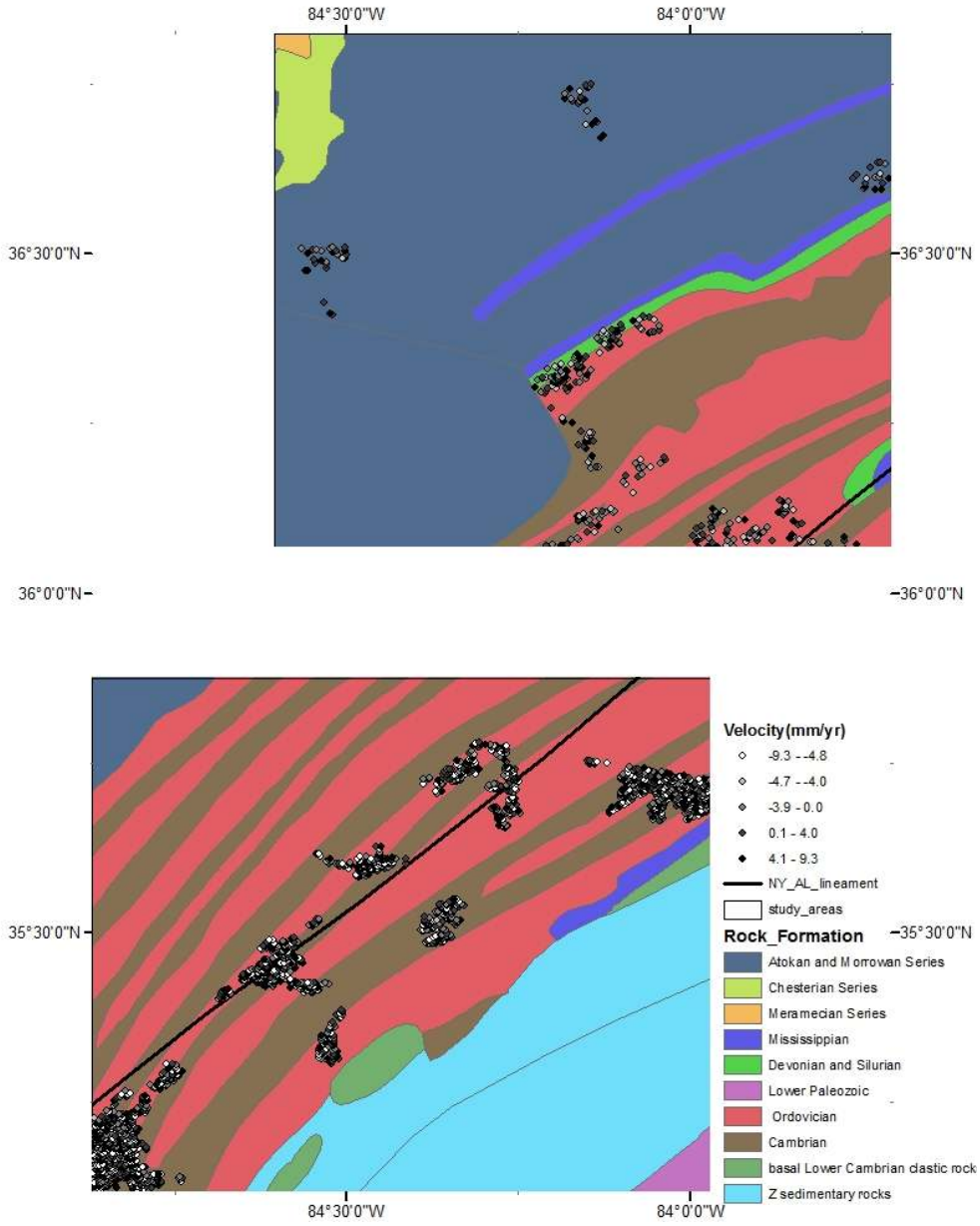

Fig. 6. Map of Velocity (mm/year) over rock types in the study areas

collapse [36]. At places where significant changes in land surface occurred due to reasons mentioned above, actual land surface deformation rate due to the seismicity are likely overestimated or compromised. To estimate actual seismicity's contribution to land surface deformation with high accuracy, there is a need to remove the land subsidence/ uplift due to erosion, groundwater overpumping and karst landscape including sinkholes in the study area.

Interpretation of findings from this study should be cautious in order to avoid inappropriate use of the complex land surface deformation in ETSZ. This is the first attempt to detect land surface deformation using Persistent Scatterers Interferometric SAR in ETSZ. Further studies are needed to investigate the surface deformation in rural areas along the NY-Alabama lineament in order to examine complete spatial pattern in deformation rate on two sides of the NY-Alabama lineament. New studies are also

needed to examine how compounding factors including erosion, groundwater withdrawal and mining influence land uplift and subsidence in this region. In addition, the impact of sinkholes on land surface in the study area needs to be investigated in order to estimate actual contribution to observed values.

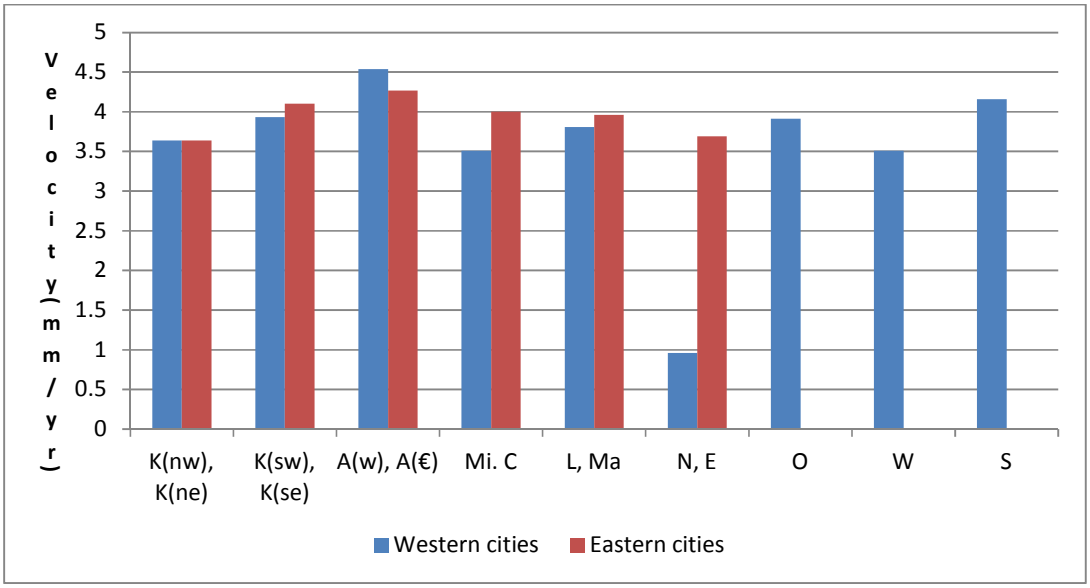

Fig. 7. Mean uplift velocity in the two sides of NY-AL lineament (K(nw): Knoxville (northwest); K(ne): Knoxville (northeast); K(sw): Knoxville (southwest); K(se): Knoxville (southeast); A(w); Athens(west); A(e); Athens(east); Mi: Middlesborough; C: Cleveland; L: La Follette;; Ma: Madisonville; N: Norris; E: Etowah; O: Oneida; W: Williamsburg; S: Sweetwater)

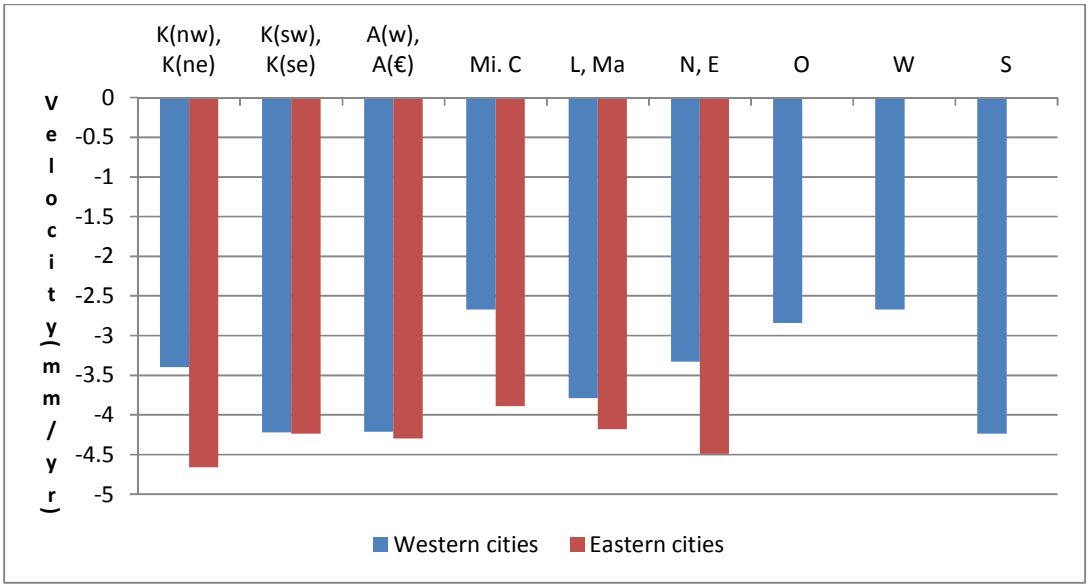

Fig. 8. Mean subsidence velocity in the two sides of NY-AL lineament (K(nw): Knoxville (northwest); K(ne): Knoxville (northeast); K(sw): Knoxville (southwest); K(se): Knoxville (southeast); A(w); Athens(west); A(e); Athens(east); Mi: Middlesborough; C: Cleveland; L: La Follette;; Ma: Madisonville; N: Norris; E: Etowah; O: Oneida; W: Williamsburg; S: Sweetwater)

Table 4. Land surface deformation in cities along two sides of NY-Alabama lineament

Name	Study area	Average velocity (mm/year)			Distance to NY-AL (km)	Position to NY-AL
		Uplift	Subsidence	Overall		
Middlesborough, KY-TN-VA	First	3.51	-2.67	1.51	31.91	Western
La Follette, TN	First	3.81	-3.79	0.21	39.98	Western
Norris, TN	First	0.96	-3.33	-2.18	23.27	Western
Oneida, TN	First	3.91	-2.84	2.01	77.35	Western
Williamsburg, KY	First	3.51	-2.67	1.31	72.15	Western
Knoxville, TN(NW)	First	3.64	-3.4	0.29		Western
Knoxville, TN(NE)	First	3.64	-4.66	1.22		Eastern
Knoxville, TN(SE)	Second	4.1	-4.24	-0.61		Eastern
Athens, TN(E)	Second	4.27	-4.3	0.28		Eastern
Cleveland, TN	Second	4	-3.89	0.25	6.38	Eastern
Madisonville, TN	Second	3.96	-4.18	-0.24	9.87	Eastern
Etowah, TN	Second	3.69	-4.49	-0.17	14.68	Eastern
Western side		3.96	-3.89	-0.04		
Eastern side		4.03	-4.07	0.19		

4. CONCLUSION

In this study, PSInSAR was successfully employed to analyze forty six ESR ½ SAR images covering two study areas with different seismic activity. After interferometric SAR analysis, spatial statistics of surface deformation velocity along line of sight was conducted using ArcGIS software to enable a comparison between two study areas and to examine the land surface deformation in cities located in the west and east of the New York-Alabama lineament.

Our results show that the average uplift and subsidence rates were lower in the first study area than in the second study area that is associated with a higher seismicity rate. Also, both average uplift and subsidence velocities were lower for cities in the first study area than for those in the second study area. In addition, surface deformation rate was higher in the second area than in the first study area regardless of rock types. These results indicate that land surface deformation including both uplift and subsidence might be mainly due to seismicity activities in both study areas. There was, however, no consistent spatial pattern in uplift or subsidence rate on either side of NY-Alabama lineament among cities. The spatial statistics shows that there were no significant differences in uplift, subsidence and overall velocity between urban areas west and east of NY-AL lineament. Thus, there was no significant relationship between the position relative to the NY-AL lineament and the land surface deformation in the study areas.

Our findings indicate that the land surface deformation in study areas was associated with the seismicity in both study areas but it was not spatially related to the NY-Alabama lineament. There is no direct association between the land surface deformation and the position relative to the NY-AL lineament in the study areas. However, interpretation of results from this study needs to be cautious since there are many factors, in addition to seismotectonic processes, that contribute to land surface deformation. They might have significant effects on deformation measurements in study areas. Geodetic measurements such as ground leveling measurements are highly suggested in the ETSZ to verify finding from this study and to identify the deformation sources. In addition, the impact of sinkholes on land surface in the study area needs to be investigated in order to have more accurate estimate of land surface deformation.

ACKNOWLEDGEMENTS

This work was partially supported by NSF grant HRD-0833184. Any opinions, findings, and conclusions or recommendations expressed in this presentation are those of the authors and do not necessarily reflect the views of the funding agencies. The authors would like to thank to the European Space Agency for providing the ERS images under the Project ID C1P-6942 and Dr. Pierre Arroucau for fruitful discussions and assistance in this research.

COMPETING INTERESTS

Authors have declared that no competing interests exist.

REFERENCES

1. Wheeler RL. Tectonic summaries for web-served earthquake responses, Southeastern North America, Open-File Report 2003-343; 2003.
   Available:http://pubs.er.usgs.gov/publication/ofr03343
   (Accessed 29 Jan 2016)
2. Powell CA, Bollinger GA, Chapman MC, Sibol MS, Johnston AC, Wheeler RL. A seismotectonic model for the 300 kilometer long eastern Tennessee seismic zone. Science. 1994;264:686-688.
3. Vlahovic G, Powell CCA, Chapman MC, Sibol MS. Joint hypocenter-velocity inversion for the eastern Tennessee seismic zone. Journal of Geophysical Research. 1998;101:8531-8542.
4. Steltenpohl MG, Zietz I, Horton JW Jr., Daniels DL. New York–Alabama lineament: A buried right-slip fault bordering the Appalachians and mid-continent North America. Geology. 2010;38(6):571-574.
5. Brown LD, Oliver JE. Vertical crustal movements from leveling data and their relation to geologic structure in the Eastern United States. Reviews of Geophysics. 1976;14:13–35.
6. Citron GP, Brown LD. Recent vertical crustal movements from precise leveling surveys in the Blue Ridge and Piedmont Provinces, North Carolina and Georgia. Tectonophysics. 1979;52:223-238.
7. Calais E, Han JY, DeMets C, Nocquet JM. Deformation of the North American plate interior from a decade of continuous GPS measurements. J. Geophys. Res. 2006;111:B06402.
   DOI: 10.1029/2005JB004253
8. Frankel A, Smalley R, Paul J. Significant motions between GPS sites in the New Madrid Region: Implications for seismic hazard. Bulletin of the Seismological Society of America. 2012;102(2):479–489.
   DOI: 10.1785/0120100219
9. Chan YK, Koo VC. An introduction to synthetic aperture radar (SAR). Progress in Electromagnetics Research B. 2008;2:27–60.
10. Colesanti C, Wasowski J. Investigating landslides with space-borne synthetic aperture radar (SAR) interferometry. Engineering Geology. 2006;88:173–199.
11. Richards MA. Beginner's guide to interferometric SAR concepts and signal processing. IEEE Georgia Institute of Technology. IEEE A&E SYSTEMS MAGAZINE. 2007;22(9):5-29.
12. Ferretti A, Prati C, Rocca F. Permanent scatteres in SAR interferometry. IEEE Transactions on Geosciences and Remote Sensing. 2001;39(1):8-20.
13. Ferretti A, Prati C, Rocca F. Non-linear subsidence rate estimation using permanent scatterers in differential SAR interferometry. IEEE Trans. Geosci. Remote Sensing. 2000;38:2202–2212.
14. Funning GJ, Bu¨rgmann R, Ferretti A, Novali F, Fumagalli A. Creep on the rodgers creek fault, northern San Francisco Bay area from a 10 year PS-InSAR dataset. Geophys. Res. Lett. 2007;34:L19306.
    DOI: 10.1029/2007GL030836
15. Massironi M, Zampieri D, Bianchi M, Schiavo A, Franceschini A. Use of PSInSAR™ data to infer active tectonics: Clues on the differential uplift across the Giudicarie belt (Central-Eastern Alps, Italy). Tectonophysics. 2009;476(1–2): 297-303.
16. Sousa JJ, Ruiz AM, Hanssen RF, Bastos L, Gil AJ, Galindo-Zaldívar J, de Galdeano CS. PS-InSAR processing methodologies in the detection of field surface deformation—study of the Granada basin (Central Betic Cordilleras, Southern Spain). Journal of Geodynamics. 2010;9(3–4):181-189.
17. Lagios E, Papadimitriou P, Novali F, Sakkas V, Fumagalli A, Vlachou K, Del Conte S. Combined seismicity pattern analysis, DGPS and PSInSAR studies in the broader area of Cephalonia (Greece). Tectonophysics. 2012;524–525:43-58.
18. Perrone G, Morelli M, Piana F, Fioraso G, Nicolò G, Mallen L, Cadoppi P, Balestro G, Tallone S. Current tectonic activity and differential uplift along the cottian Alps/Po plain boundary (NW Italy) as derived by PS-InSAR data. Journal of Geodynamics. 2013;66:65-78.
19. Huang M, Bürgmann R, Pollitz F. Lithospheric rheology constrained from twenty-five years of postseismic deformation following the 1989 Mw 6.9 Loma Prieta earthquake. Earth and Planetary Science Letters. 2016;435:147-158.

20. Bollinger GA, Johnston AC, Talwani P, Long LT, Shedlock KM, Sibol MS, Chapman MC. Seismicity of the southeastern United States; in Neotectonics of North America, Decade Map Col. 1, D.B. Slemmons, E.R. Engdahl, M.D. Zoback, and D.D. Blackwell (Editors), Geological Society of America, Boulder, Colorado; 1991.
21. Hatcher RD, Bream Jr. BR, Merschat AJ. Tectonic map of the southern and central Appalachians: A tale of three orogens and a complete Wilson cycle. Mem. Geol. Soc. Am. 2007;200:595–632.
22. Wheeler RL. Earthquakes and the the craton wide limit of Iapetan faulting in eastern North America, Geology. 1995;23: 105-108.
23. Dunn MM. Relocation of Eastern Tennessee Earthquakes Using hypoDD, 2004;4-6.
24. Cook FA, Albaugh DS, Brown LD, Kaufman S, Oliver JE, Hatcher Jr. RD. Thin-skinned tectonics in the crystalline Southern Appalachians; COCORP seismic reflection profiling of the blue ridge and piedmont. Geology. 1979;7:563-567.
25. Zoback MD, Zoback ML. Tectonic stress field of North America and relative plate motions, in Slemmons DB., Engdahl, E.R., Zoback, M.D. and Blackwell, D.D., eds., Geotectonic of North America. Geol. Soc. Amer., Decade Map, Boulder, Co. 1991;1:563-567.
26. Longwell TJ, Parks WL, Springer ME. University of Tennessee Agricultural Experiment Station, moisture characteristics of tennessee soils. Bulletins; 1963.
Available:http://trace.tennessee.edu/utk_agbulletin/303
(Accessed on May 9, 2016)
27. Turnage KM, Lee SY, Foss JE, Kim KH, Larsen IL. Comparison of soil erosion and deposition rates using radiocesium, RUSLE and buried soils in dolines in East Tennessee. Environmental Geology. 1997; 29 (1/2):1-9.
28. Xu H, Zhou Y, Li C. Analysis and simulation of spaceborne SAR interferometric baseline. In Proceedings of the CIE International Conference on Radar, Beijing, China. 2001;639–643.
29. Tu J, Gu D, Wu Y, Dongyun D. Error modeling and analysis for InSAR spatial baseline determination of satellite formation flying. Mathematical Problems in Engineering. 2012;Article ID 140301:23. Available:http://dx.doi.org/10.1155/2012/140301
30. Bamler R. Digital terrain models from radar interferometry. Photogrammetrische Week. 1997;93-105.
31. Exelis Visual Information Solutions. 2010. ENVI 4.8/SARscape 5.0. Boulder, Colorado: Exelis Visual Information Solutions.
32. ESRI 2011. ArcGIS Desktop: Release 10. Redlands, CA: Environmental Systems Research Institute.
33. McDonald JH. Handbook of Biological Statistics Sparky House Publishing, Baltimore; 2008.
34. Cheng J, Wu J, Zhang L, Zou J, Liu G, Zhang R, Yu B. Deformation Trend Extraction Based on Multi-Temporal InSAR in Shanghai, Remote Sens. 2013;5:1774-1786.
DOI: 10.3390/rs5041774
35. Mével HL, Feigl KL, Córdova l, DeMets C, Paul Lundgren C. Evolution of unrest at Laguna del Maule volcanic field (Chile) from InSAR and GPS measurements, 2003 to 2014. Geophysical Research Letters. 2015;42(16):6590–6598.
DOI: 10.1002/2015GL064665
36. Kohl MS. Subsidence and sinkholes in East Tennessee: A field guide to holes in the ground. Division of Geology Public Information Series no. 1, State of Tennessee Department of Environment and Conservation, Nashville, TN. 2001;14.
37. Kettle RH, Newton JG, Tanner JM, LaMoreaux PE. Karst subsidence in East Tennessee. Report from Oak Ridge National Laboratory; 1986.
Available:http://info.ngwa.org/gwol/pdf/880149704.pdf
(Accessed on Jan 20, 2016)
38. Denton P. Tennessee soil erosion picture fuzzy. Southeast Farm Press; 2000. Available:http://southeastfarmpress.com
(Accessed on Nov 29, 2015)
39. Nearing MA, Norton LD, Bulgakov, DA, Larionov GA, West LT, Dontsova KM. Hydraulics and erosion in eroding rills. Water Resources Research. 1997;33(4): 865-876.
40. Blanco-Canqui H, Lal R. Soil and water conservation. Principles of soil

conservation and management. Dordrecht: Springer. 2008;54–80.
ISBN 9781402087097

41. Willett SD, Hovius N, Brandon MT, Fisher DM. Tectonics, climate and landscape evolution. Geological Society of America Special Papers. 2006;398:vii-xi.
DOI: 10.1130/2006.2398(00)

42. Wilson AM, Gorelick S. The effects of pulsed pumping on land subsidence in the Santa Clara Valley, California. J. Hydrol. 1996;174:375–396.

43. Galloway DL, Burbey TJ. Review: Regional land subsidence accompanying groundwater extraction. Hydrogeol. J. 2011;19:1459–86.

Peer-review history:
The peer review history for this paper can be accessed here:
http://sciencedomain.org/review-history/15267